Modeling and simulation of bone cells dynamic behavior under the late effect of breast cancer treatments

Imane Ait Oumghar, Abdelwahed Barkaoui, Abdellatif El Ghazi, Patrick Chabrand

Modeling and simulation of bone cells dynamic behavior under the late effect of breast cancer treatments

Imane Ait Oumghar [a,b], Abdelwahed Barkaoui [a,*], Abdellatif EL Ghazi [c], Patrick Chabrand [b]

[a] Université Internationale de Rabat, LERMA Lab, Rocade Rabat Salé 11100, Rabat-Sala El Jadida, Morocco
[b] Université Aix-Marseille, ISM, 163 av. de Luminy F-13288, Marseille cedex 09, France
[c] Université Internationale de Rabat, TIC Lab, Rocade Rabat Salé 11100, Rabat-Sala El Jadida, Morocco

A B S T R A C T

Breast Cancer (BC) treatments have been proven to interfere with the health of bones. Chemotherapy and endocrinal treatment regimens such as tamoxifen and aromatase inhibitors are frequently prescribed for women with BC. However, these drugs increase bone resorption and reduce the Bone Mineral Density (BMD), thus increasing the risk of bone fracture. In the current study, a mechanobiological bone remodeling model has been developed by coupling cellular activities, mechanical stimuli, and the effect of breast cancer treatments (chemotherapy, tamoxifen, and aromatase inhibitors). This model algorithm has been programmed and implemented on MATLAB software to simulate different treatment scenarios and their effects on bone remodeling and also predict the evolution of Bone Volume fraction (BV/TV) and the associated Bone Density Loss (BDL) over a period of time. The simulation results, achieved from different combinations of Breast Cancer treatments, allow the researchers to predict the intensity of each combination treatment on BV/TV and BMD. The combination of chemotherapy, tamoxifen, and aromatase inhibitors, followed by the combination of chemotherapy and tamoxifen remain the most harmful regimen. This is because they have a strong ability to induce the bone degradation which is represented by a decrease of 13.55% and 11.55% of the BV/TV value, respectively. These results were compared with the experimental studies and clinical observations which showed good agreement. The proposed model can be used by clinicians and physicians to choose the most appropriate combination of treatments, according to the patient's case.

1. Introduction

Bone disorders occur as a result of different types of diseases and their treatment regimens [1]. Cancer, for example, is considered to be one of the pathologies that massively affect the bone mass. It can impact the turnover of the bone and cause its dysregulation through several complex biological interactions with bone cells' osteoblasts (OB), osteoclasts (OC), and osteocytes (OCY) during Bone Remodeling (BR) process [2]. In addition, the existing treatments that are devoted to these types of diseases induce bone mass degradation and increase the risk of fractures from 10% to 20% [3,4]. Fractures occur as a result of reducing Bone Mineral Density (BMD) in some skeletal areas such as the spine, hip, and wrist [5]. In the medical field, different procedures are used based on the type of cancer and are independent of each other such as surgery, radiotherapy, and chemotherapy. However, some interventions should be implemented based on the specifics of the cancer diagnosed.

In case of Breast Cancer, the intervention method depends on the stage of the disease, age of the patient and the histological grade of the tumor [6,7]. Two types of cancer treatment are combined together as given herewith; (i) local treatments (e.g., lumpectomy, mastectomies, tenonectomies) and (ii) systemic treatments (e.g. radiation therapy, chemotherapy, endocrine or hormone therapy and targeted therapy) [8].

Before starting the treatment procedure, the breast cancer is diagnosed at first based on biopsy. To increase the accuracy of the diagnosis, the biopsy is generally accompanied by medical imaging and clinical examination [9]. There are four steps followed in the treatment strategy for women with primary and secondary breast cancer such as the surgery, radiotherapy, chemotherapy and hormonal therapy. At first, in surgical procedure, either a radical removal of the breast is performed or else a breast-conserving procedure is conducted. Nowadays, the Breast-Conserving Surgery (BCS) is increasingly being adopted [10],

given its principle of leaving the healthy tissue and removing only the tumor mass and its surrounding parts. BCS is generally performed, when the tumor has not widely invaded the breast and the adjacent organs. After performing this surgery, radiotherapy is conducted to kill the remaining masses of the tumor, left after the operation [11]. On the other hand, the surgery could also be preceded by radiography in order to shrink the tumor and facilitate the removal of the tissues (ii) Radiotherapy involves the direct delivery of high doses of radiation to the tumor cells [12]. This procedure allows the reduction of cancer mass and the local recurrence rates followed by the increased rate of survival among the patients with early-stage cancer [13]. (iii) Chemotherapy involves drugs that are capable of destroying the cancer cells. These medications could be administered either intravenously or orally. This procedure is highly efficient in case of breast Estrogen Receptor (ER) negative tumors [14]. Yet, it is also used for almost all types of breast cancers, most importantly TNBC, HER2+, and high-risk luminal tumors [9]. It has also become the main treatment procedure followed for advanced breast cancer cases. Further, radiotherapy and chemotherapy allow tumor shrinkage and are used as neoadjuvant therapies after surgery. (iii) Hormonal therapy is considered to be an adjuvant therapy, especially used for hormone-sensitive breast cancer. Several hormone therapy drugs are available that aim at preventing the integration of estrogen (E) and ER complex since this binding has an important role in promoting the growth of the breast cancer [15].

From radiotherapy, chemotherapy to hormone therapy, the overall set of methods that are dedicated to heal the cancer induce bone degradation which persists even after the recovery process [16]. At a macroscopic level, radiotherapy has been found to induce fragile fractures within a period of a few months to years, after the treatment. In terms of microscopic level, radiotherapy decreases the cellularity and marrow adiposity, affects the proliferation and differentiation of OB, and their production of collagen, and increases the OC differentiation, when using low doses of radiation [17]. Chemotherapy has been shown to increase the number of OCs by increasing the inflammatory cytokine concentration and decreasing the Wnt/β-catenin signaling pathway activation, which in turn promotes the OB differentiation, and induces the OCY apoptosis [18]. In terms of hormone therapy, two types of hormone therapy are of special interest as given herewith; (i) the tamoxifen and (ii) aromatase inhibitors. Both treatments act on estrogen, which stimulates the bone formation over the BR cycle. Tamoxifen exerts agonist and/or antagonist effect on the estrogen-to-estrogen receptor binding [19]; whereas the aromatase inhibitors reduces the concentration of estrogen from nearly 52% to 98% by preventing the aromatase enzyme activity i.e., the conversion of rest of the hormones to estrogen [20].

Several numerical models have been developed to simulate the biological and mechanical responses of the bone cells and their impact on bone quality [21–24]. Based on those models, many researchers investigated the efficacy of treatments and provided a long-term prediction of their effects [25,26]. Yet, to the best of the authors' knowledge, only a few studies have attempted to evaluate the effects of cancer treatments upon the bone quality.

In this scenario, the aim of the current research work is to predict the BC treatments' effect on BR using the widely-applied Pharmacokinetic Pharmacodynamic (PK/PD) model approach [27,28]. The model has been implemented in such a way that the pathology mechanism and the effect of drug administration and elimination become possible [29,30]. Two types of treatments are considered in this work: (i) chemotherapy, and (ii) hormone therapy, composed of tamoxifen and aromatase inhibitors. The chemotherapy effect was incorporated by enhancing the formation of OC and OB cells followed by the degradation of the cancerous cells. Further, Tamoxifen and aromatase inhibitors' effects were also incorporated by reducing the E-ER binding and osteoprotegerin (OPG) concentrations that stimulate the bone formation process.

2. Modeling of combined BC treatments

2.1. Mechanobiological BR model

The goal of this study is to combine the effect of BC treatments, with the biochemical pathway in BR, so as to determine the OB and OC activity at the BMU level (Fig. 1). The behavior of the bone cells is also controlled by the mechanical stimulation in order to represent the cells' adaptation to external loadings. In the following section, an extension of the model [31] is represented that incorporates the effect of BC cells and the bone cells' responses to mechanical stimulation, on the remodeling process. The model parameters are presented in (Table 2) and the formulations of osteoblast precursors (OB_p), active osteoblast (OB_a), and active osteoclasts (OC_a) behaviors are presented herewith.

$$\begin{cases} \dfrac{dC_{OBp}(t)}{dt} = D_{OBu}\pi_{act}^{OBu\rightarrow OBp}C_{OBu} + \mathscr{P}_{OBp}\Pi_{act,OBp}^{mech}C_{OBp} - D_{OBp}\pi_{rep,TGF\beta}^{OBp\rightarrow OBa}C_{OBp} \end{cases} \tag{1}$$

$$\begin{cases} \dfrac{dC_{OBa}(t)}{dt} = D_{OBp}\pi_{rep,TGF\beta}^{OBp\rightarrow OBa}C_{OBp} - A_{OBa}C_{OBa} \end{cases} \tag{2}$$

$$\begin{cases} \dfrac{dC_{OCa}(t)}{dt} = D_{OCp}\pi_{act,[RANK.RANKL]}^{OCp\rightarrow OCa}C_{OCp} - A_{OCa}\pi_{act,TGF\beta}^{OCa\rightarrow +}C_{OCa} \end{cases} \tag{3}$$

Here, C_{OBu}, C_{OBp}, C_{OBa}, C_{OCp} and C_{OCa} correspond to the uncommitted osteoblasts (OBu), OBp, OBa, preosteoclasts (OCp), and OCa concentrations respectively whereas D_{OBu}, D_{OBp}, and D_{OCp} correspond to the differentiation rates of OBu, OBp, and OCp respectively. $\mathscr{P}_{OBp}$ denotes the maximum proliferation rate of OBp, A_{OBa}, and A_{OCa} correspond to OBa and OCa apoptosis rates respectively. In case of behaviors of the osteoblasts, $\pi_{act}^{OBu\rightarrow OBp}$ and $\pi_{rep,TGF\beta}^{OBp\rightarrow OBa}$ denote the hill functions that represent the ability of the Transforming Growth Factor beta (TGF_β) and wingless (Wnt) respectively, to stimulate the natural differentiation of OBu into OBp and the ability of TGF_β to inhibit the natural differentiation of OBp into OBa. For osteoclasts' behavior, $\pi_{act,[RANK.RANKL]}^{OCp\rightarrow OCa}$ and $\pi_{act,TGF\beta}^{OCa\rightarrow +}$ denote the hill functions representing the ability of the receptor activator of NF-kB (RANK) and receptor activator of NF-kB ligand (RANKL) binding to promote the preosteoclats' differentiation and the ability of the TGF_β to stimulate the apoptosis of the active osteoclasts. Finally, $\Pi_{act,OBp}^{mech}$ is a function that represents the ability of mechanical strains to promote the proliferation of preosteoblasts described in detail in the literature [32–34]. The concentration of RANK-RANKL, used for $\pi_{act,[RANK.RANKL]}^{OCp\rightarrow OCa}$ calculation, depends on the actions of many biochemical factors, whether those secreted by osteoblasts or those secreted by BC cells in the bone microenvironment, such as osteoprotegerin, parathyroid hormone (PTH), parathyroid hormone-related protein (PTHrP), interleukin 6 (IL-6), and dickkopf-related protein 1 (DKK-1).

The Hill activation and the repression functions, used in the model, are expressed as $\pi_{act} = \frac{C_X}{K_{act,X}+C_X}$ in case of activation and as $\pi_{rep} = \frac{K_{rep}}{K_{rep,X}+C_X}$ in case of repression.

(Table 1) resumes all the biochemical factors involved in the RANK-RANKL concentration. Here, each factor X, β_X: production rate, $\widetilde{D_X}$: degradation rate, C_X : concentration of X, C_{Xmax} : concentration maximum de X, $K_{a,X}$: association binding rate of its ligand, and $K_{act,X}$and $K_{rep,X}$:association and repression Hill constants are used respectively for the studied factors and Hill functions. For Wnt production, it depends on the time at which the Wnt production rate increases, because of the cancer $t_{Wnt}$and the duration of this increase τ_{Wnt} [35].

$\pi_{act}^{OBu\rightarrow OBp}$, π_{RANKL}^{Ligand}, and π_{OPG}^{Ligand} expressions depend on the synergistic effects that result from the interaction of the biochemical factors involved in the process [31,36].

For TGFβ, Wnt, and DKK-1:

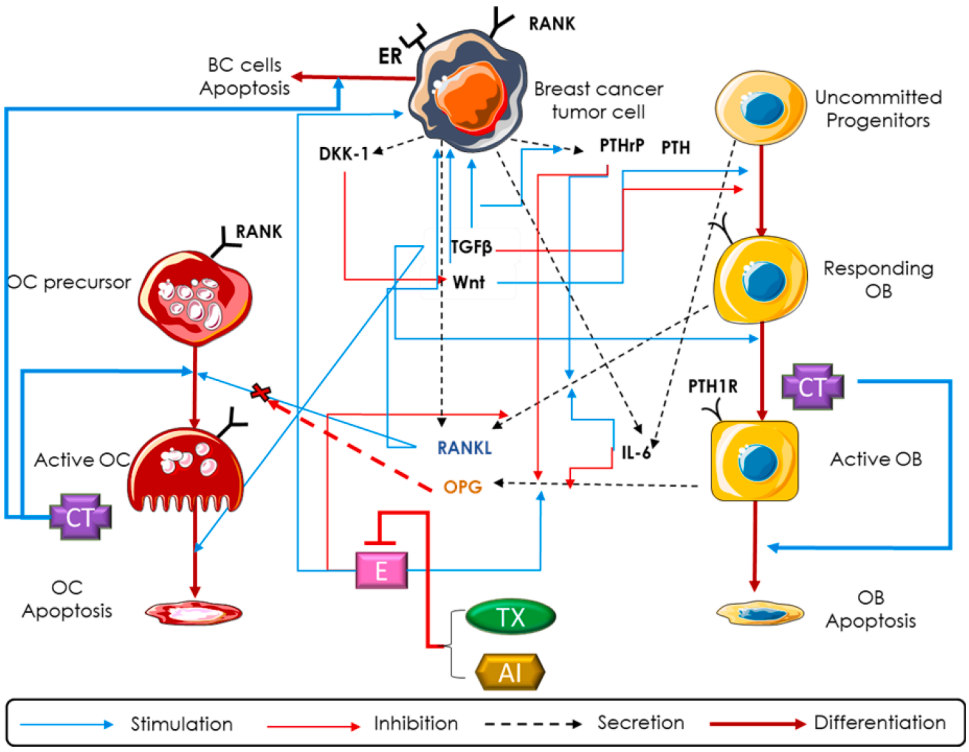

Fig. 1. Schematical representation of the BC tumor cells' interactions with bone cells in bone microenvironment during BR process, in the presence of BC treatments. Chemotherapy (CT) acts on the viability of OBa OCa, and BC cells whereas tamoxifen (TX) and aromatase inhibitors (AI) act by limiting the involvement of estrogen in BR.

- TGFβ and Wnt stimulate the differentiation of OBu into OBp.
- TGFβ cytokine constitutes a large amount of bone matrix constituent factors. Thus, it depends on the amount of bone resorbing cells.
- DKK-1, secreted by OBa, inhibits the production of Wnt using $\pi_{rep,DKK1}$.

For RANK/RANKL/OPG:

- The concentration of RANK-RANKL complex, upon the pre-osteoclasts $C_{OCp,[RANK.RANKL]}$, depends on RANK concentration $C_{OCp,RANK}$ and RANKL concentration C_{RANKL}.
- $C_{OCp,RANK}$ is considered to be proportional to the concentration of the osteoclast precursors as each cell has a fixed number of RANK receptor, $\rho_{OCp,RANK}$.
- $C_{RANKL}$is determined based on the mass action kinetics principle explained in the literature [37].Here, $C_{RANKLmax}$ denotes the maximum RANKL concentration and C_{OPG} corresponds to OPG concentration.
- According to the current study authors, the maximum RANKL in the microenvironment is 100% expressed by OBp and is controlled by the Hill function, π_{RANKL}^{Ligand}.
- C_{OPG} value depends on active osteoblasts and is regulated by the Hill function, π_{OPG}^{Ligand}.

For PTH, IL-6 and E

- RANKL, released by the OBp, is stimulated by PTH and IL-6 and inhibited by Estrogen
- OPG, released by the OBa, is stimulated by Estrogen and inhibited by PTH and IL-6
- PTH and IL-6 concentrations are determined based on the principle of mass action kinetics. The PTH concentration depends on the concentration of PTHrP, secreted by tumor cells whereas the IL-6 concentration depends on its production by OBu and tumor cells.
- Estrogen concentration is supposed to be a constant value during one of the remodeling processes and its value for healthy women is equal to $8.151 \times 10pM$ [38].

For the mechanical stimulus

- The function, representing the mechanical stimulus $\Pi_{act,OBp}^{mech}$, depends on Strain Energy Density (SED) is noted as Ψ_{bm}. Here, λ denotes the strength of the biomechanical transduction of bone formation and Ψ_{bm} is a function of the applied stress that is expressed as Σ. SED is expressed as follows, $\Psi_{bm} = \frac{1}{2}\varepsilon_{bm} : c_{bm} : \varepsilon_{bm}$ in which c_{bm} denotes the bone matrix stiffness tensor of the human femur and ε_{bm} corresponds to the microscopic strain that gets generated in bone extracellular matrix. ε_{bm} is determined based on the homogenization procedure detailed in the literature [33]. In this procedure, it has been shown that Ψ_{bm} depends on the stress tensor Σ and the vascular porosity $(1 - BV/TV)$.
- When the SED value is below the minimum value $\Psi_{bm}(t_0)$, $\Pi_{act,OBp}^{mech} = \frac{1}{2}$ decreases the proliferation rate of the preosteoblasts whereas if the SED exceeds its maximal value $\widehat{\Psi_{bm}}$, the mechanical stimulus becomes equal to 1. This results in the maximum proliferation of the preosteoblasts.
- The SED effect on the production of RANKL is also implemented through the function P_{RANKL}^{mech}, which in turn reflects the ability of mechanical disuse $(\Psi_{bm} < \Psi_{bm}(t_0))$ to promote RANKL production and completely inhibit it, when $(\Psi_{bm} \geq \Psi_{bm}(t_0))$. This function depends on the parameter α that represents the inhibition parameter.

The concentrations of Wnt, DKK-1, IL-6, and PTH depend on the concentration of BC cells while the latter is determined using the following equation.

Table 1
Biochemical regulation functions and the mechanical stimulus that controls the BR process under BC effect in the proposed model [31].

Factor	Function	Factor concentration
TGFβ	$\pi_{act}^{OBu\rightarrow OBp} = (\pi_{act,TGF\beta}^{OBu\rightarrow OBp} + \pi_{act,Wnt}^{OBu\rightarrow OBp}) + (\pi_{act,TGF\beta}^{OBu\rightarrow OBp}\pi_{act,Wnt}^{OBu\rightarrow OBp})$	$C_{TGF\beta} = \frac{\alpha k_{res} C_{OCa}}{\widetilde{D_{TGF\beta}}}$
Wnt		$C_{Wnt} = \frac{(\beta_{Wnt} + \beta_{Wnt,T} C_T)\pi_{rep,DKK1}}{\widetilde{D_{Wnt}}}$
		$\beta_{Wnt,T} = \beta_{Wnt,T}^{max} \frac{e^{(t-t_{Wnt})/\tau_{Wnt}} + \beta_{Wnt,T}^{min}/\beta_{Wnt,T}^{max}}{e^{(t-t_{Wnt})/\tau_{Wnt}} + 1}$
DKK-1		$C_{DKK1} = \frac{\beta_{DKK1,T} C_T}{\widetilde{D_{DKK1}}}$
RANK/RANKL/OPG	$\pi_{act,[RANK.RANKL]}^{OCp\rightarrow OCa} = \frac{C_{OCp,[RANK.RANKL]}}{K_{act,[RANK.RANKL]}^{OCp\rightarrow OCa} + C_{OCp,[RANK.RANKL]}}$	$C_{OCp,[RANK.RANKL]} = K_{a,[RANK.RANKL]} C_{RANKL} C_{OCp,RANK}$ $C_{OCp,RANK} = \rho_{OCp,RANK} C_{OCp}$ $C_{RANKL} = \frac{C_{RANKLmax}}{(1 + K_{a,OPG} C_{OPG} + K_{a,RANK} C_{OCp,RANK})} \left(\frac{\beta_{OBp,RANKL} + \beta_{T,RANKL} + P_{RANKL}^{mech}}{\beta_{OBp,RANKL} + \widetilde{D_{RANKL}} C_{RANKLmax}}\right)$ $C_{RANKLmax} = (R_{RL,OBp} C_{OBp} + R_T C_T)\pi_{RANKL}^{Ligand}$ $C_{OPG} = \frac{(\beta_{OBa,OPG} C_{OBa})\pi_{OPG}^{Ligand}}{\frac{(\beta_{OBa,OPG} C_{OBa})\pi_{rep,OPG}^{Ligand}}{C_{OPGmax}} + \widetilde{D_{OPG}}}$ $P_{RANKL}^{mech} = \begin{cases} \alpha\left(1 - \frac{\Psi_{bm}}{\Psi_{bm}(t_0)}\right), & \Psi_{bm} < \Psi_{bm}(t_0) \\ 0 & \Psi_{bm} \geq \Psi_{bm}(t_0) \end{cases}$
PTH, IL-6	$\pi_{RANKL}^{Ligand} = (\pi_{act,RANKL}^{PTH} + \pi_{act,RANKL}^{IL6} + \pi_{rep,RANKL}^{E}) + (\pi_{act,RANKL}^{PTH}\pi_{rep,RANKL}^{E}) - (\pi_{act,RANKL}^{PTH}\pi_{act,RANKL}^{IL6})$ $\pi_{OPG}^{Ligand} = (\pi_{rep,OPG}^{PTH} + \pi_{rep,OPG}^{IL6} + \pi_{act,OPG}^{E}) + (\pi_{rep,OPG}^{PTH}\pi_{act,OPG}^{E}) - (\pi_{rep,OPG}^{PTH}\pi_{rep,OPG}^{IL6})$	$C_{PTH} = \frac{\beta_{PTH} + \beta_{PTHrP} C_T \pi_{act,TGF}^{PTHrP}}{\widetilde{D_{PTH}}}$ $C_{IL6} = \frac{(\beta_{IL6} C_{OBu} + \beta_{IL6,T} C_T)\pi_{act,TGF}^{IL6}}{\frac{(\beta_{IL6} C_{OBu} + \beta_{IL6,T} C_T)\pi_{act,TGF}^{IL6}}{C_{IL6max}} + \widetilde{D_{IL6}}}$ $C_E = 8.151 \times 10 pM$
Mechanical	$\Pi_{act,OBp}^{mech} = \begin{cases} 0 & \Psi_{bm} \leq \Psi_{bm}(t_0) \\ \frac{1}{2}\left(1 + \lambda\left(\frac{\Psi_{bm}}{\Psi_{bm}(t_0)} - 1\right)\right)^{\frac{1}{2}}, & \Psi_{bm}(t_0) < \Psi_{bm} \leq \widehat{\Psi_{bm}} \\ 1 & \widehat{\Psi_{bm}} \leq \Psi_{bm} \end{cases}$	$\Psi_{bm} = \Psi_{bm}(\Sigma, c_{bm}, (1 - BV/TV))$ $\widehat{\Psi_{bm}} = (1 + \lambda^{-1})\Psi_{bm}(t_0)$

$$\frac{dC_T(t)}{dt} = P_T \pi_{act}^{E} ln\left(\frac{C_{Tmax}}{C_T}\right) C_T \tag{4}$$

C_T denotes the BC concentration, C_{Tmax} corresponds to the maximum concentration of the BC cells, P_T denotes the proliferation rate of the metastatic BC cells, and π_{act}^{E} corresponds to the Hill activation function of the cancer cells that undergo proliferation by estrogen.

The fraction of the extravascular bone matrix i.e., BV/TV behavior is determined using the Eq. (4). BV/TV depends on the concentration of active osteoblasts and osteoclasts whereas k_{form} and k_{res} represent the daily volumes of the bone matrix formed by osteoblast and the daily volume of bone matrix resorbed by the osteoclast.

$$\frac{dBV/TV(t)}{dt} = \left(k_{form} C_{OBa} - k_{res} C_{OCa}\right) \tag{5}$$

The proposed model promotes the evolution of BV/TV (Eq. (5)). Since it is an established fact that the bone mass change, under BC treatment, is usually reported in terms of BMD, the authors exhibited concerns to determine the relative change of bone mass for comparative purposes using Bone Density Loss (BDL) as a percentage (Eq. (5)).

$$\text{BDL} = \frac{BV/TV(t_0) - BV/TV(t)}{BV/TV(t_0)} \tag{6}$$

3. PK-PD models

3.1. Treatments doses

Chemotherapy: For chemotherapy, the treatment period was considered to be 4 months during when the chemotherapy drug was taken once for every 3 weeks. Chemotherapy dose D_{ch} depends on the type of drug used for the treatment. In this study, the authors considered $40 mg/m$ dosage for the ixabepilone treatment [39]. This type of chemotherapy drug is generally used to treat the patients with metastatic breast cancer and have developed resistance to taxanes and anthracyclines [40].

Tamoxifen and Aromatase inhibitor: For tamoxifen dose D_{Tx}, the treatment duration was 3 years with a daily dose of $20mg$ [41]. While, for the aromatase inhibitor, specifically exemestane dose D_{AI}, the treatment duration was considered to be 2 years with a daily dose of $25mg$ and starts after tamoxifen period [42]. In general, Exemestane is also used for metastatic breast cancer, specifically for ER positive type of tumor cells and it works on reducing the estrogen amount in the body [43].

3.2. PK models

In order to implement the drugs' effect on bone remodeling process, the authors opted for PK-PD models. In this section, the authors define the PK models of chemotherapy, tamoxifen, and the aromatase inhibitor. The parameters used in the PK models were obtained from the literature, [44,45], and [46] for chemotherapy, tamoxifen, and aromatase inhibitors, respectively (Table 3).

Chemotherapy: The concentration of the chemotherapy drug, in blood plasma, was determined based on the standard PK model described earlier [47], including the continuous dosage rate of chemotherapy drug $D_{ch}(t)$. The PK model of ixabepilone treatment is expressed as follows:

$$\frac{dC_{Ch}(t)}{dt} = k_{a,Ch} D_{Ch} - k_{e,Ch} C_{Ch} \tag{7}$$

Where, $D_{Ch} = m_{Ch}/M_{Ch}$, C_{Ch} denotes the concentration of ixabepilone in blood plasma, and $k_{a,Ch}$ and $k_{e,Ch}$ correspond to absorption and

elimination rates of ixabepilone by the blood respectively.

Tamoxifen: The concentration of Tamoxifen drug in blood plasma was determined based on a general one compartment PK model as described earlier [48] (Eq. (8)). In this model, the administration of the tamoxifen in blood and its elimination were included, by considering its washout by the body and its transformation to 4-OH Tamoxifen and NH Tamoxifen.

$$\frac{dC_{Tx}(t)}{dt} = k_{a,Tx}\frac{m_{Tx}}{M_{Tx}}\frac{F_{Tx}}{V_{d,Tx}} - \left(k_{12,Tx} + k_{13,Tx} + k_{e,Tx}\right)C_{Tx} \tag{8}$$

Here, m_{Tx} denotes the mass of the tamoxifen assimilated by the patient, M_{Tx} denotes the molar mass of tamoxifen, $V_{d,Tx}$ corresponds to the volume of tamoxifen administration, F_{Tx} is the tamoxifen bioavaibility constant, $k_{a,Tx}$ is the administration rate of tamoxifen, $k_{12,Tx}$ and $k_{13,Tx}$ denote the tamoxifen transformation rates into N-desmethyl-tamoxifen and 4-hydroxy-tamoxifen respectively, and finally $k_{e,Tx}$ is the elimination rate of tamoxifen.

$$\frac{dC_{AI}(t)}{dt} = k_{a,AI}\frac{m_{AI}}{M_{AI}}\frac{F_{AI}}{V_{d,AI}} - \left(k_{12,AI} + k_{13,AI} + k_{e,AI}\right)C_{AI} \tag{9}$$

Where, m_{AI} is the mass of the aromatase inhibitor assimilated by the patient, M_{AI} is the molar mass of the aromatase inhibitor, $V_{d,AI}$ is the volume of tamoxifen administered into the body, F_{AI} is the bioavaibility constant, $k_{a,AI}$ is the administration rate of aromatase inhibitor, $k_{12,AI}$ and $k_{13,AI}$ denote the transfer of aromatase inhibitor to other organs/compartments rates respectively, and finally $k_{e,AI}$ is the elimination rate of aromatase inhibitor.

3.3. PD models

In terms of PD models, the parameters used were obtained from the literature [49,50], and [51] for chemotherapy, tamoxifen, and aromatase inhibitors respectively (Table 3).

Chemotherapy: As mentioned in the introduction, in addition to its effect on cancer cells, the chemotherapy method strongly affects the osteoblasts and osteoclasts. To represent its effect, the authors also included the killing efficacy functions, pertaining to alter the concentrations of the bone cells and breast cancer cells, both during and after the end of the treatment Eqs. (10)–(12).

$$\varepsilon_T(t) = v_T\left(\left(1 - e^{-x_T C_{Ch}}\right) + \alpha_T\left(1 - e^{-\frac{t}{tf}}\right)\right) \tag{10}$$

$$\varepsilon_C(t) = v_C\left(\left(e^{-x_O C_{Ch}} - 1\right) + \alpha_O\left(1 - e^{-\frac{t}{tf}}\right)\right) \tag{11}$$

$$\varepsilon_B(t) = v_B\left(\left(e^{-x_O C_{Ch}} - 1\right) + \alpha_O\left(1 - e^{-\frac{t}{tf}}\right)\right) \tag{12}$$

ε_T, ε_C and ε_B denote the efficacy of chemotherapy on BC cells, osteoclasts, and osteoblasts respectively and t_f is the total duration of the simulation. The total duration was fixed to be 7 years which is inclusive of 2 years after the treatment is over. Those equations are composed of two main terms, the first one represents the ability of chemotherapy to kill the cells based on the concentration of chemotherapy and the second term represents the late killing effect of chemotherapy that lasts after the treatment is over. This second term allows the apoptosis of the cells, even after the end of the treatment.

v_B, v_C and v_T denote the kill rate of osteoblasts, osteoclasts and cancer cells respectively whereas $x_T$and x_O correspond to the chemotherapeutic efficacy rate on cancer and bone cells respectively. Finally, α_T and α_O denote the controlling factors of chemotherapy that exhibits late effect on the tumor cells and bone cells respectively.

Based on the above discussion, the new 'bone remodeling and BC cancer model' under chemotherapy is expressed as follows.

$$\frac{dC_{OBa}(t)}{dt} = D_{OBp}\pi^{OBp\to OBa}_{rep,TGF\beta}C_{OBp} - A_{OBa}C_{OBa} - \varepsilon_B C_{OBa} \tag{13}$$

$$\frac{dC_{OCa}(t)}{dt} = D_{OCp}\pi^{OCp\to OCa}_{act,[RANK.RANKL]}C_{OCp} - A_{OCa}\pi^{OCa\to +}_{act,TGF\beta}C_{OCa} - \varepsilon_C C_{OCa} \tag{14}$$

$$\frac{dC_T(t)}{dt} = P_T\pi^E_{act}ln\left(\frac{C_{Tmax}}{C_T}\right)C_T - \varepsilon_T C_T \tag{15}$$

Tamoxifen and Aromatase inhibitor: The effect of the hormonal therapies on estrogen is given in the following equations.

$$C_{[\mathrm{ER.E}]} = K_{a,[\mathrm{ER.E}]}C_{ER}C_E \tag{16}$$

$$C_{ER} = \rho_{ER}C_{OBa} \tag{17}$$

$$C_E = \frac{C_{Emax}}{\left(1 + K_{a,[\mathrm{Tx.E}]}C_{Tx}\delta + K_{a,[\mathrm{ER.E}]}C_{ER}\right)}\left(\frac{\beta_E}{\beta_E + \widetilde{D_E}C_{Emax}}\right) \tag{18}$$

$$C_{Emax} = C_{Eb}\pi^E_{rep} \tag{19}$$

$$S^E_{rep,TX} = 1 - \frac{C_{Tx} - C_{Txmax}}{C_{Txmin} - C_{Txmax}} \tag{20}$$

$$\pi^E_{rep,AI} = \left(\frac{K_{rep,AI}}{C_{AI} + K_{rep,AI}}\right)^{0.8} \tag{21}$$

$C_{[\mathrm{ER.E}]}$, C_E and C_{ER} denote the E-ER concentration, E concentration and ER concentration respectively. $S^E_{rep,TX}$ and $\pi^E_{rep,AI}$ correspond to the efficacy function of tamoxifen and the Hill repression function of the aromatase inhibitors on E production correspondigly. $K_{a,[\mathrm{ER.E}]}$ and $K_{a,[\mathrm{Tx.E}]}$ denote the association binding constants of E-ER and E-Tamoxifen respectively while $K_{rep,AI}$ corresponds to the Hill repression constant of the aromatase inhibitors, ρ_{ER} is the number of ER expressed by OBa, δ is the factor of tamoxifen binding to estrogen, β_E and $\widetilde{D_E}$ denote the production and the degradation rates of E respectively and C_{Emax} and C_{Txmax} are the maximum concentrations of E and tamoxifen correspondingly. C_{Txmin} is the minimum concentration of tamoxifen.

The late effect of both tamoxifen and aromatase inhibitors is represented by the OPG production rate of osteoblasts as given below.

$$\beta_{OPG}(t) = \begin{cases} \beta_{OBa,OPG}\left(\lambda_{Tx}\dfrac{e^{-\frac{t}{tf}}}{e^{-\frac{t}{tf}} + 1}\right) \text{ if } C_{Tx} \neq 0 \\ \beta_{OBa,OPG}\left(\lambda_{AI}\dfrac{e^{-\frac{t-t_{AI}}{tf}}}{e^{-\frac{t-t_{AI}}{tf}} + 1}\right) \text{ if } C_{AI} \neq 0 \\ \beta_{OBa,OPG} \text{ if } C_{Tx} = C_{AI} = 0 \end{cases} \tag{22}$$

$\beta_{OBa,OPG}$ is the production rate of OPG by active osteoblasts, λ_{Tx} and λ_{AI} denote the OPG decreasing factors due to tamoxifen and aromatase respectively and t_{AI} is the time at which the patient starts to undergo the aromatase inhibitors treatment.

3.4. Validation of the PK model

In this study, the authors simulate and calibrated the PK model for chemotherapy, tamoxifen, and aromatase inhibitors on the basis of literature [44–46]. In this paper, the authors considered that the initial concentration of all the studied treatments remain null. During each iteration of the calculation, a new drug dose was administrated following the treatment protocol mentioned in (Section 2.2). For the sake of validation, the models were simulated based on the experimental parameters, for a short period of time, in order to compare the outcomes with experimental observation. Fig. 2 represents the concentration behavior of both chemotherapy (Ixabepilone) as well as the aromatase inhibitors (Exemestane), obtained by the proposed model along with

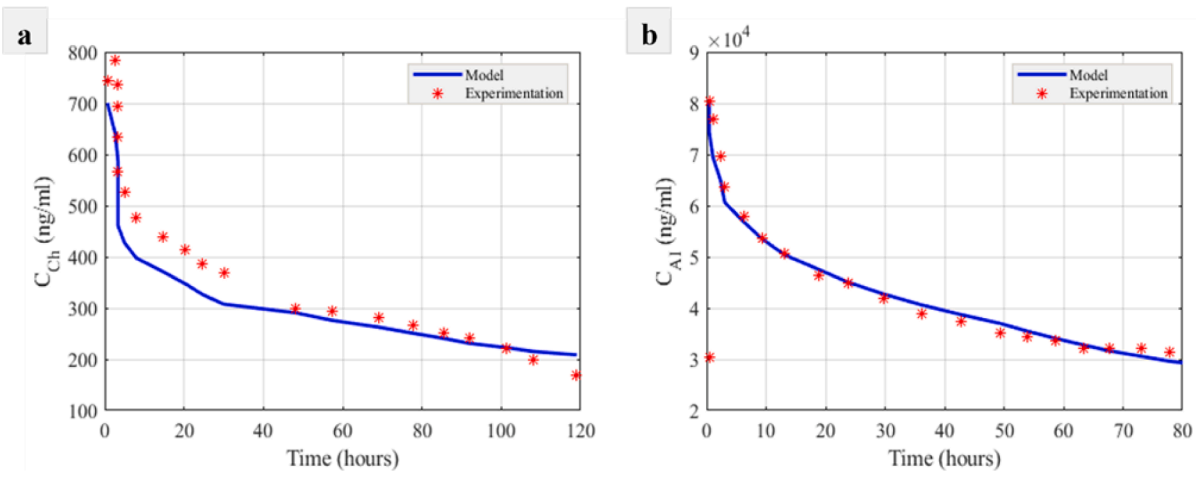

Fig. 2. Comparison of concentrations between (a) chemotherapy (Ixabepilone) and (b) aromatase inhibitors (Exemestane) obtained by the proposed model with experimentation from literature.

experimentation from the literature [44] and [46] over 120 and 80 h respectively. A good agreement was found between the numerical and the experimental behavior of chemotherapy and aromatase inhibitor treatments. For tamoxifen oral drugs, [45] the authors did not provide plasma concentration of tamoxifen over a period of time. Yet, according to the results [45], the tamoxifen concentrations at the steady state was

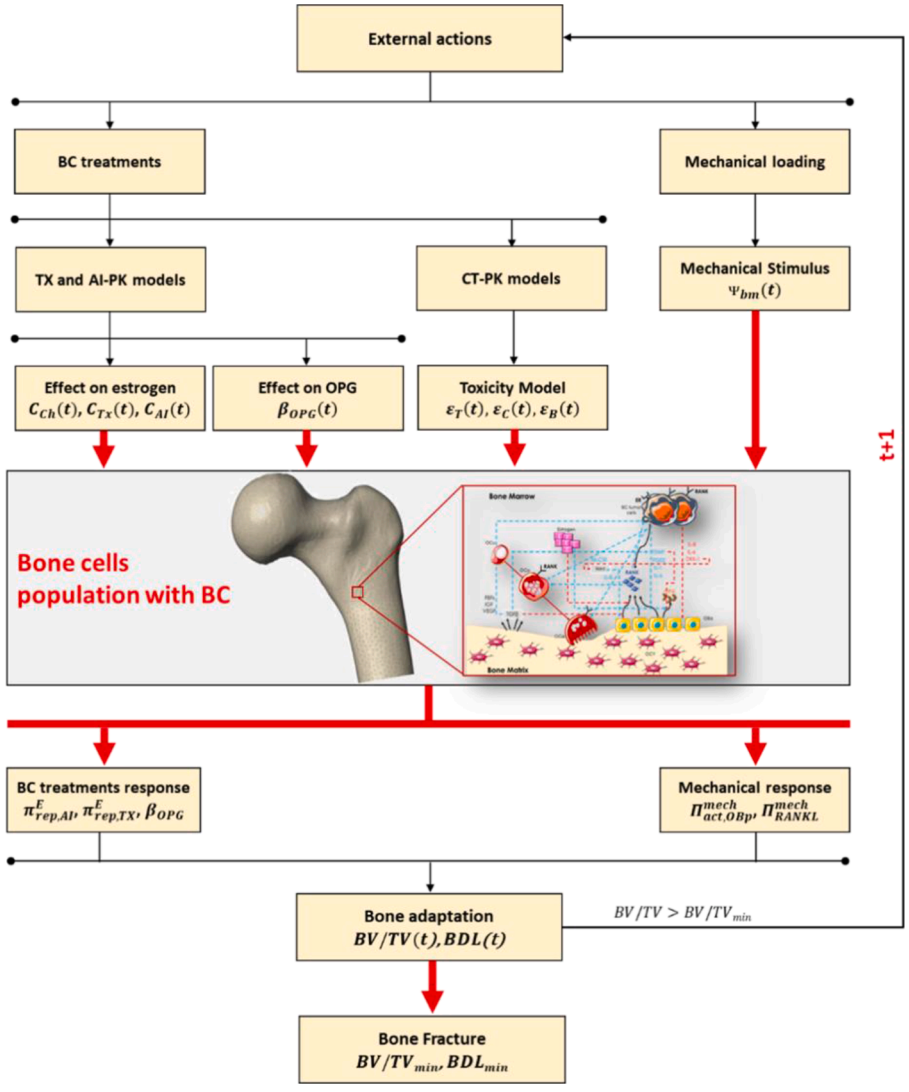

Fig. 3. Schematic representation of the algorithmic formulation for the proposed model, implemented in MATLAB.

$\approx$ 200*ng/ml*, which align with that of the current study results.

3.5. Algorithmic model formulation

The presented model was implemented by taking two driving inputs into consideration i.e., (i) the PK models of chemotherapy, tamoxifen, and aromatase inhibitors, and (ii) their mechanical loadings. In PK model, the drugs were permitted to impact the bone cells behavior either directly or through estrogen involvement. On the other hand, the mechanical stimuli affected the bone cells through $\Pi^{mech}_{act.OBp}$ and P^{mech}_{RANKL} functions. The resultant BV/TV value, controlled by the bone cells, closes the mechanical feedback loop (Fig. 3) as it permits to update the SED-stimulating bone cells. The PK models were calibrated based on the literature [44–46] whereas the BR model was calibrated under normal conditions by taking new parameter values into consideration such as WNT, DKK-1, IL-6 and E involvement as in the literature [31]. Both BR and the PK/PD differential equations models were resolved using a diurnal timescale over 7 years to represent the whole duration of the treatment along with a supplementary period of 2 years after the cessation of intake treatments. The equations of the proposed model were programmed on MATLAB and all the dynamic behaviors of drugs and cells were calculated using numerical integration by the fourth order Runge-Kutta method.

4. Results

In order to investigate the effectiveness of the proposed model and predict the effect of BC treatment on bone quality, the authors analyzed different configurations of the combined treatments on women with BC.

4.1. Combined BC treatments

Based on the knowledge gained earlier that different configurations of treatments are suggested for patients suffering from BC, the authors investigated the usage of different configurations of the treatments in the current study. The BV/TV values were determined for four different treatment configurations such as (i) BC+ chemotherapy (BC+CT), (ii) BC+ chemotherapy+ tamoxifen (BC+CT+TX), (iii) BC+ chemotherapy+ tamoxifen+ aromatase inhibitors (BC+CT+TX+AI), and (iv) BC+ tamoxifen+ aromatase inhibitors (BC+TX+AI) (Fig. 4a).

Compared to normal conditions, the BV/TV values got reduced after BC emergence and reached a steady state after 6 months of time. During the period, the total bone loss was found to be 12.62%. When the patient started undergoing BC treatment, the bone reacted differently based on the treatments prescribed to them. There was a decline in the BV/TV values for all the studied configurations with variated concentrations as given herewith. (i) 13.55% with chemotherapy combined with tamoxifen and aromatase inhibitors, (ii) 11.55% with chemotherapy combined with tamoxifen, (iii) 10.15% with only chemotherapy, and (iv) 1.74% with only hormone therapies. The outcomes were in concordance with the experimental findings reported in the literature i.e., the BMD values of the amenorrhoeic patient get reduced, when they are provided with chemotherapy in multiple parts of the skeleton such as the lumbar spine and the proximal femur either during [52] or after ceasing the chemotherapy [53]. Concerning the hormone therapies, it has reported that the BMD losses were significantly higher when using the aromatase inhibitors than when using the tamoxifen [54]. This inference has been represented by the proposed model which showed less BV/TV with the addition of aromatase inhibitors.

With regards to aromatase inhibitors used after chemotherapy, sequentially after 2–3 years of tamoxifen, a decline of 2.6–3.5% BMD was observed with exemestane in lumbar spine after 1 to 2 years of treatment [54]. This finding aligns with the result that showed a 4.8% increase of BDL after starting exemestane in a chemotherapy+ tamoxifen+ aromatase inhibitors configuration.

Besides the BV/TV value, the mechanical stimulus of the BR also got affected by the treatment configuration, as it depends on the bone quality. As presented in (Fig. 4b), the SED values got increased simultaneously over a period of time to bone degradation. However, the SED values were found to be moderately increasing over time for all the

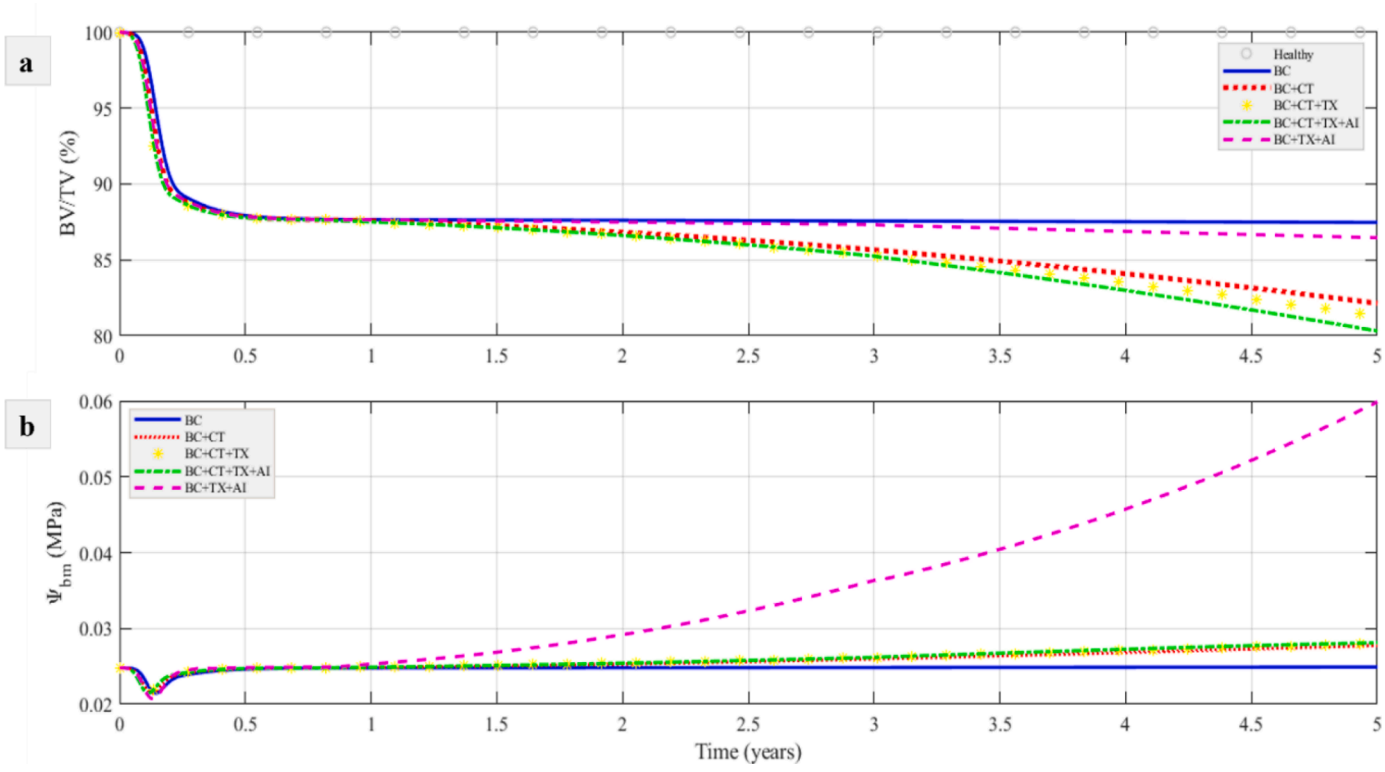

Fig. 4. (a) BV/TV changes and (b) SED values over a period of five years in a patient with BC under different configurations of treatment.

treatment configurations, except the hormone therapy. Indeed, by using tamoxifen followed by aromatase inhibitors, the SED values experienced a 2.41-fold increase, thus allowing a heavy stimulation of the bone forming cells. In the literature [55], the authors have investigated the effect of tamoxifen on trabecular bone mechanical loading and the volume and structure of the cortical bone. According to the outcomes, the ER modulators such as tamoxifen were found to have enhanced the bone response to mechanical loading process. The findings are in concordance with the outcomes of the proposed model. The use of chemotherapy in the proposed model was found to be more powerful in inhibiting the anabolic effect of the tamoxifen than the effect of aromatase inhibitors.

In addition to the drugs' impact on the bone, the proposed model permitted the authors to provide the efficacy of each treatment configuration in BC killing process (Fig. 5).

In this study, the authors considered a very low concentration of the BC cells, as an initial condition of BC model calculation (Table 2) and also considered the surgical procedure, which was applied before undergoing chemical treatments. Based on the model outcomes, it can be inferred that a combination of chemotherapy, tamoxifen, and aromatase inhibitors, followed by a combination of chemotherapy and tamoxifen, is the most effective treatment regimen in eradicating the cancer cells.

4.2. *BC treatments doses effect*

For the purpose of investigating each and every treatment effect in a separate manner, the proposed model was simulated in which only one treatment type was taken into account with varying concentrations. Fig. 6 shows the BDL evolution for all the three treatments under different dosages.

The repetitive tests, conducted in the study, demonstrated that an increase in the chemotherapy dose results in further loss of the important bone density compared to hormone therapy. The dosage of Tamoxifen had a moderate and slow effect on the bone development whereas the aromatase inhibitors had a highly recognizable effect i.e., it significantly increased with an increase in the dosage. When those treatments were compared, the BDL increase was found to be quite linear under chemotherapy, but non-linear under hormone therapy. For instance, a 2-fold increase in chemotherapy dose induced a 12.83% BDL increase and a 3-fold increase induced a further 10.6% BDL increase. Further, a 2-fold increase in tamoxifen induced a 0.73% BDL increase whereas a 3-fold dose increase induced only a 0.16% BDL increase.

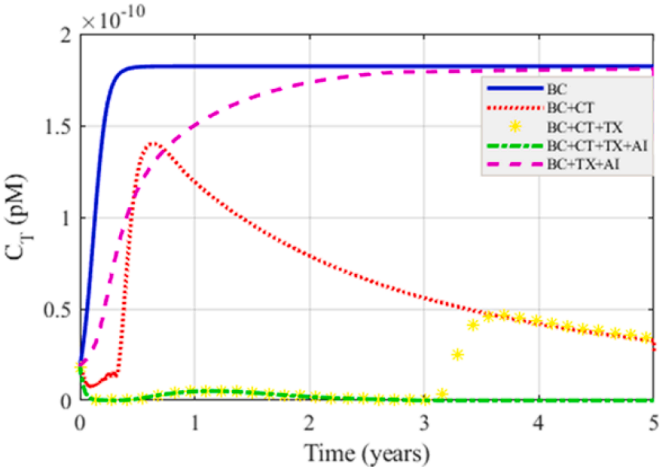

Fig. 5. Concentration of BC cells over five years under different configurations of the treatment.

5. Discussion

In the current research work, the authors implemented the catabolic effects of different BC treatments on bone remodeling. The study evaluated the effects of chemotherapy, tamoxifen, and aromatase inhibitors with the help of PK/PD modeling method. The late effect of those treatments was also invested, whether by direct action on the bone cells' concentration – chemotherapy – case or through controlling the OPG production by osteoblasts – tamoxifen and aromatase inhibitors – cases. Chemotherapy stimulated the degradation of the OBa and cancer cells while stimulating the growth of OCa. With regards to tamoxifen and aromatase inhibitors, they controlled the E-ER concentration given the agonist and antagonist effects of the tamoxifen and the ability of aromatase inhibitors to limit the production of estrogen. Besides, the late effect of those treatments was mediated by limiting the production of OPG to reflect the osteolysis. In terms of direct effect of the chemotherapy on bone cells, (Fig. 7) depicts the impact of chemotherapy on enhancing and hastening the growth of OCa while stimulating the degradation of OBa.

The concentration of OCa was found to have been accelerated in addition to low acceleration of OBa concentration, either after BC occurrence or after adding the effect of chemotherapy. However, during the chemotherapy process, the increase of osteoclasts was found to be higher over the entire period, before reaching the steady state. On the other hand, the concentration of the osteoblasts got increased for the first 2.5 months after which it got reduced below its value in case of BC only. Besides, while converging to steady state, both OCa and OBa converged at higher and lower concentrations respectively, than the control case. This behavior, exhibited by both OCa and OBa, was in concordance with the expectations of the authors, as it reflects the additional effect of chemotherapy on bone cells' behavior. Further, the results also consequently reflect the decreased BV/TV value after undergoing chemotherapy, as presented in (Fig. 4a).

The simulation results (Fig. 8) represent the pharmacodynamic effect of tamoxifen, followed by aromatase inhibitors, on E-ER concentration. It indicates that a daily dosage of 20 mg of tamoxifen and 25 mg of aromatase inhibitors induce around 2.5-fold and 8.51-fold reduction of E-ER concentration respectively. This outcome meet the experimental findings thus confirming that tamoxifen induces the reduction of estradiol 2 in the plasma [56]. Further, the aromatase inhibitors are highly effective in influencing the concentration of estrogen [20], which directly affects the E-ER concentration. The reduction in the E-ER concentration results in indirect promotion of the osteoclastogenesis, given the main role of estrogen in suppressing the RANKL production and promoting the OPG production. RANK/RANKL/OPG pathway is the lead controller of bone cells' behavior. Due to RANKL action, the catabolic action is highly pronounced.

The BDL value was calculated after 2 years of discontinuing the type of treatment used earlier. This was done to predict the late effect of the treatments on bone quality. (Table 4) shows the percentage of bone density loss obtained from the simulation. Those outcomes were compared with the observations on BMD loss percentage, reported in the literature, for different parts of the bone.

The current study results are consistent with those in the literature. Vehmanen et al. [53] determined the late effect of chemotherapy on bone loss and found the BMD loss of 5.1% and 6.1% in the femoral neck and 10.4% and 10.5% in the lumbar spine of women, with amenorrhea and with normal menopause, respectively. In literature [59], Hadji et al. found 5.6% and 10.3% BMD loss in femoral neck and lumbar spine respectively. These findings show that women menstruation and the skeletal area play an important role in predicting the bone loss percentage. In case of tamoxifen effect, the literature has reported that it induces BMD loss after the end of treatment. This phenomenon endangers 1–2% of loss per year in both proximal femur and lumbar spine for the non-postmenopausal women [54]. For postmenopausal women, the authors found a 5.2% BMD loss in the lumbar spine after 2–3 years of

Table 2
Bone remodeling model parameters under breast cancer effect.

Parameter	Value	Description	Reference
C_{OBu}	$3.27 \times 10^{-6} pM$	OBu concentration	[31]
$C_{OBp,ini}$	$7.67 \times 10^{-4} pM$	OBp initial concentration	[31]
$C_{OBa,ini}$	$6.39 \times 10^{-4} pM$	OBa initial concentration	[31]
C_{OCp}	$1.28 \times 10^{-3} pM$	OCp concentration	[31]
$C_{OCa,ini}$	$1.07 \times 10^{-4} pM$	OCa initial concentration	[31]
D_{OBu}	$2.646 \times 10^{2} 1/day$	Differentiation rate of OBu	[31]
D_{OBp}	$4.65 \times 10^{-1} 1/day$	Differentiation rate of OBp	[31]
D_{OCp}	$4.097 1/day$	Differentiation rate of OCp	[31]
$AptCommandmathbfcalP_{OBp}$	$5.01 \times 10^{2} 1/day$	Proliferation rate of OBp	[31]
A_{OBa}	$3.91 \times 10^{-1} 1/day$	Apoptosis rate of OBa	[31]
A_{OCa}	$1.21/day$	Apoptosis rate of OCa	[31]
$\widetilde{D_{RANKL}}$	$4.161/day$	Degradation rate of RANKL	[31]
$\widetilde{D_{PTH}}$	$3.84 \times 10^{2} 1/day$	Degradation rate of PTH	[31]
$\widetilde{D_{OPG}}$	$4.161/day$	Degradation rate of OPG	[31]
$\widetilde{D_{DKK1}}$	$0.15251/day$	Degradation rate of DKK-1	[31]
$\widetilde{D_{Wnt}}$	$21/day$	Degradation rate of Wnt	[31]
$\widetilde{D_{IL6}}$	$4.99 \times 10^{1} 1/day$	Degradation rate of IL-6	[31]
$\beta_{DKK1,T}$	$1.09 \times 10^{5}\ 1/day$	Production rate of DKK-1 by tumor cells	[31]
β_{Wnt}	$9 \times 10^{-3} pM/day$	Intrinsic production rate of Wnt by OB	[31]
$\beta^{min}_{Wnt.T}$	$5 \times 10^{3}\ 1/pM$	Minimum production rate of Wnt by tumor	[31]
$\beta^{max}_{Wnt.T}$	$1 \times 10^{4}\ 1/pM$	Maximum production rate of Wnt by tumor	[31]
β_{PTH}	$9.74 \times 10^{2} pM/day$	Intrinsic production rate of PTH	[31]
β_{PTHrP}			[31]
$\beta_{OBp,RANKL}$	$1.62 \times 10^{2} pM/day$	Production rate of RANKL by OBp	[31]
$\beta_{T,RANKL}$	$3.83 \times 10^{-8}\ pM/day$	Production rate of RANKL by tumor cells	[31]
β_{IL6}	$3.16 \times 10^{4}\ 1/day$	IL6 production by OBu per day	[31]
$\beta_{IL6,T}$	$8.4 \times 10^{3}\ 1/day$	IL6 production by tumor cell per day	[31]
$\beta_{OBa,OPG}$	$1.63 \times 10^{8} 1/day$	Production rate of OPG by OBa	[31]
$K^{OBu \to OBp}_{act.TGF\beta}$	$4.28 \times 10^{-4} pM$	Activation coefficient of OBu differentiation controlled by TGF_β	[31]
$K^{OBp \to OBa}_{rep.TGF\beta}$	$2.49 \times 10^{-4} pM$	Repression coefficient of OBp differentiation controlled by TGF_β	[31]
$K^{OCa \to +}_{act.TGF\beta}$	$4.28 \times 10^{-4}\ pM$	Activation coefficient of OCa apoptosis controlled by TGF_β binding to its receptor	[31]
$K^{IL6}_{act.TGF\beta}$	$4.28 \times 10^{-4} pM$	Activation coefficient related to TGF_β binding to its receptor	[31]
$K_{act,PTH}$	$2.09 \times 10^{2} pM$	Activation coefficient related to PTH binding to its receptor	[31]
$K_{rep,PTH}$	$2.21 \times 10^{-1} pM$	Repression coefficient related to PTH binding to its receptor	[31]
$K_{act,DKK1}$	$2.09 \times 10^{4} pM$	Activation coefficient related to DKK-1 binding to its receptor	[31]
$K_{rep,DKK1}$	$4.28 \times 10^{-4} pM$	Repression coefficient related to DKK-1 binding to its receptor	[31]
$K_{act,Wnt}$	$1.74 \times 10^{5} pM$	Activation coefficient related to Wnt binding to its receptor	[31]
$K_{act,IL6}$	$2.525 \times 10^{4} pM$	Activation coefficient related to IL-6 binding to its receptor	[31]
$K_{rep,IL6}$	$2.525 \times 10^{4} pM$	Repression coefficient related to IL-6 binding to its receptor	[31]
$K_{act,E}$	$9.2307 \times 10^{2} pM$	Activation coefficient related to estrogen binding to its receptor	[31]
$K_{rep,E}$	$2.1 \times 10^{2} pM$	Repression coefficient related to estrogen binding to its receptor	[31]
$K^{OCp \to OCa}_{act.[RANK.RANKL]}$	$4.79 \times 10^{1} pM$	Activation coefficient related to RANKL binding to its receptor RANK	[31]
$K_{A2,RANK}$	$7.19 \times 10^{-2} 1/pM$	Association binding constant RANK-RANKL	[31]
$K_{A1,OPG}$	$5.68 \times 10^{-2} 1/pM$	Association binding constant OPG-RANKL	[31]
C_{OPGmax}	$7.98 \times 10^{2} pM$	Maximum OPG concentration	[31]
C_{IL6max}	$8.01 \times 10^{-1} pM$	Maximum concentration of IL-6	[31]
$R_{RL,OBp}$	3×10^{6}	Maximum number of RANKL expressed by OBp	[31]
R_T	4.06×10^{4}	Maximum number of RANKL expressed by tumor cells	[31]
$\rho_{OCp,RANK}$	10, 000	Fixed number on OCp surface	[31]
$\frac{\alpha k_{res} C_{OCa}}{\widetilde{D_{TGF\beta}}}$	1	α: TGF_β content stored in the bone matrix $\widetilde{D_{TGF\beta}}$: Degradation rate of TGF_β	[31]
C_E	$9.175 \times 10^{1} pM$	Estrogen concentration in healthy women	[31]
k_{form}	$3.34 \times 10^{1} \%/pM.day$	Bone formation rate	[31]
k_{res}	$2 \times 10^{2} \%/pM.day$	Bone resorption rate	[31]
t_{Wnt}	$200 day$	time of increase in Wnt production	[35]
τ_{Wnt}	$50 day$	duration of increase in Wnt production	[35]
$C_{T,ini}$	$1.82 \times 10^{-11}\ pM$	Breast cancer tumor cells initial concentration	[31]
C_{Tmax}	$1.82 \times 10^{-10}\ pM$	Breast cancer tumor cells initial concentration	[31]
P_T	$0.31/pM$	Breast cancer tumor cells proliferation rate	[31]
λ	0.1	strength of biomechanical transduction of bone formation	[34]
α	$1 \times 10^{5} pM/day$	strength of biomechanical transduction of bone resorbtion	[34]
Σ	$-30 MPa$	Macroscopic stress tensor	[34]

(*continued on next page*)

Table 2 (*continued*)

Parameter	Value	Description	Reference
c_{bm}	$\begin{pmatrix} 18.5 & 10.3 & 10.4 & 0 & 0 & 0 \\ 10.3 & 20.8 & 11.0 & 0 & 0 & 0 \\ 10.4 & 11.0 & 28.4 & 0 & 0 & 0 \\ 0 & 0 & 0 & 12.9 & 0 & 0 \\ 0 & 0 & 0 & 0 & 11.5 & 0 \\ 0 & 0 & 0 & 0 & 0 & 9.3 \end{pmatrix}$	Bone matrix stiffness tensor of human femurs	[34]

Table 3
Pharmacokinetic and pharmacodynamic models' parameters for chemotherapy, tamoxifen, and aromatase inhibitors.

	Chemotherapy			*Tamoxifen*			*Aromatase inhibitor*		
	Parameter	*Value*	*Description*	*Parameter*	*Value*	*Description*	*Parameter*	*Value*	*Description*
Pharmacokinetic	m_{Ch}	40 mg/m^2	mass of the ixabepilone	m_{Tx}	20 mg	mass of the tamoxifen	m_{AI}	25 mg	mass of the aromatase inhibitor
	M_{Ch}	506, 69 g/mol	molar mass of ixabepilone	M_{Tx}	371.5 g/mol	molar mass of tamoxifen	M_{AI}	296, 403 g/mol	molar mass of aromatase inhibitor
	$k_{a,Ch}$	$6.93 \times 10^{-2} 1/h$	absorption rate of ixabepilone	$k_{a,Tx}$	0.7 $1/h$	administration rate of tamoxifen	V_{AI}/F_{AI}	844L	volume of tamoxifen administration/ bioavaibility constant
	$k_{e,Ch}$	$9.6 \times 10^{-3} 1/h$	elimination rate of ixabepilone	$k_{12,Tx}$	7.07×10^{-3} $1/h$	tamoxifen transformation rates into N-desmethyl-tamoxifen	$k_{a,AI}$	$1.13 \times 10^{-2} 1/h$	administration rate of aromatase inhibitor
				$k_{13,Tx}$	5.49×10^{-5} $1/h$	tamoxifen transformation rates into 4-hydroxy-tamoxifen	$k_{12,AI}$	$9.08 \times 10^{-3} 1/h$	Aromatase inhibitor transfer rate into the other organs
				$k_{e,Tx}$	8×10^{-3} $1/h$	elimination rate of tamoxifen	$k_{13,AI}$	3.48×10^{-3} $1/h$	Aromatase inhibitor transfer rate into the other organs
				V_{Tx}/F_{Tx}	724 L	volume of tamoxifen administration /tamoxifen bioavaibility	$k_{e,Tx}$	1.47×10^{-2} $1/h$	elimination rate of aromatase inhibitor
Pharmacodynamic	v_T	$9 \times 10^2 1/day$	kill rate of cancer cells	ρ_{ER}	1000	ER number expressed by OBa	$K_{rep,AI}$	22.1pg/ml	Repression constant of aromatase inhibitors
	v_C	$1.8 \times 10^2 1/day$	kill rate of osteoclasts	β_E	1.95×10^2 pM/day	Production rate of estrogen	λ_{AI}	3.3×10^{-4}	OPG decreasing factor due to aromatase inhibitors
	v_B	90 $1/day$	kill rate of osteoblasts	$\widetilde{D_E}$	0.01 $1/day$	Degradation rate of estrogen			
	x_O	$1.32 \times 10^3 1/mol.\ L$	chemotherapeutic efficacy rate on cancer and bone cells	C_{Eb}	54.86 pg/ml	Initial maximum concentrations of estrogen			
	α_c	0.3	maximum factor of chemotherapy late effect on tumor cells	δ	0.001	factor of tamoxifen binding to estrogen			
	α_O	0.1	maximum factor of chemotherapy late effect on bone cells	$K_{a,[ER.E]}$	1.083 $1/pM$	association binding constants of E-ER			
				$K_{a,[Tx.E]}$	$4.5 \times 10^6 1/M.s$	association binding constants of E-Tx			
				λ_{Tx}	0.1	OPG decreasing factor due to tamoxifen			

Aromatase inhibitor: The concentration of the Aromatase inhibitor drug in blood plasma was determined based on general four-compartment PK model described earlier [48] (Eq. (9)). The model is inclusive of the administration of the aromatase inhibitor in blood, its delivery from the central compartment to other three compartments followed by its natural elimination by the body.

tamoxifen treatment [57]. In terms of sequentially using the aromatase inhibitors after chemotherapy, after 2–3 years of tamoxifen, a decline of 7% in lumbar spine and 6.6% in total hip were observed after using the exemestane [54]. By excluding the chemotherapic effect, tamoxifen followed by exemestane exhibited a slight decline in the BMD value, reaching up to 0.8–1% of BMD loss based on the skeletal region under study [58].

With the model proposed in the current study, it is possible to mix many drugs at the same time and study different combinations of drugs and their impact on bone quality. Further, it is possible to determine the relationship between each drug and BDL loss by varying the dose of each drug taken. For instance, in case of aromatase inhibitors (Fig. 6), the authors found that their impact on BDL got reduced after a certain threshold. This can be attributed to the reason that once the minimum concentration of estrogen is reached, it could have an impact on the bone remodeling process. Besides, the proposed model further permitted the authors to predict the late effects of chemotherapy, tamoxifen, and aromatase inhibitors concurrently, to experimental and clinical

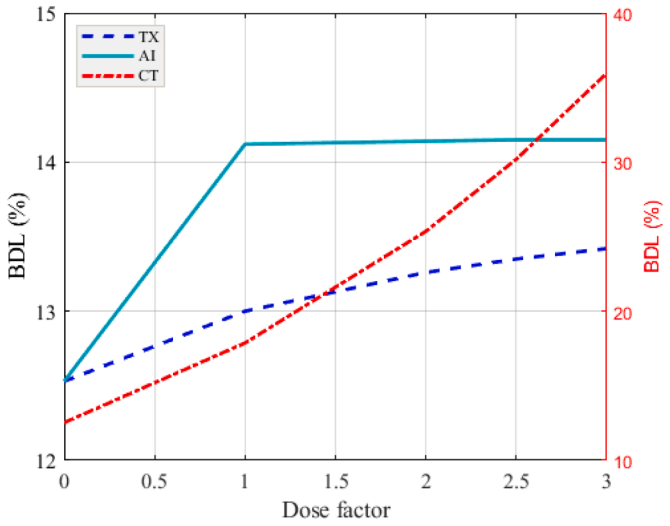

Fig. 6. BDL changes for different treatment doses factors.

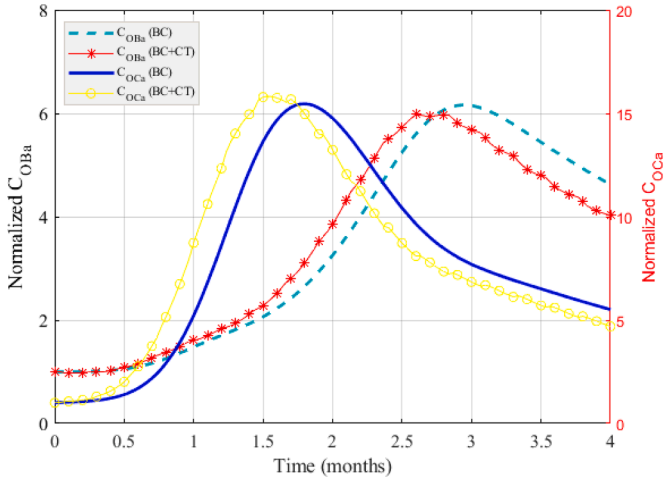

Fig. 7. OBa and OCa normalized concentration during 4 months of treatment without and with chemotherapy.

observations (Table 4).

For a better analysis of the obtained results, the authors have investigated the effect of a few parametric changes on bone remodeling model and to be specific, upon BV/TV values after 7 years.

In the current study, the authors focused on the parameters that control the late effect of chemotherapy of tamoxifen and aromatase inhibitor, on the model. For chemotherapy case, the authors observed the changes in v_C, v_B, x_O, α_O, and α_c respectively. By applying small variations, the authors found no significant variations in the v_C, v_B, and x_O upon BV/TV. For example, a 4-times increase in the v_C and v_B values led to approximately 0.01% reduction whereas a 20-times increase of x_O led to approximately 0.12% reduction. These results confirm that the concentration of the chemotherapy drug's value remains the main controlling factor in reducing the BV/TV value during the treatment.

On the other hand, for α_O and α_c parameters, a significant variation was found in the BV/TV value as shown in (Fig. 9**a,b**). The increase in both α_O and α_c values lead to a noticeable progressive decrease in the bone volume fraction. This decrease reached 13.7% after 4-times increase in the α_O value (Fig. 9**a**), while it reached 50.4% after only 4-times increase in the α_c value (Fig. 9**b**). Such outcomes confirm that the concentration of α_c controlling osteoclasts has a strong impact on the model than the concentration of α_O controlling osteoblasts. Thus, the modeling of various phenomenon could be realized only by focusing on (Eq. (3)).

For tamoxifen and aromatase inhibitor cases, the authors observed that a small variation can be attained by varying the λ_{Tx} value, which is manifested by an increase in the bone loss after decreasing its value. With regards to λ_{AI}, its effects on the BV/TV values were barely noticeable. Either λ_{Tx} and λ_{AI} controls the production of OPG, which has a significant impact on the bone remodeling process. When a minimum OPG production is attained, the BV/TV converges to a steady state, thus allowing a repression of excessive resorption, after the end of treatment. Thus, the proposed model can mimic small variations observed in the BMD values clinically (Table 4).

6. Conclusion

The current study has been devoted to investigating the effect of different BC treatments, with different configurations and doses, on bone quality. Aside from their effect on the bone, the efficacy of those treatments in limiting the BC cell development after the surgery was also investigated. Based on the outcomes achieved by the proposed model, it can be concluded that a combination of chemotherapy, tamoxifen, and aromatase inhibitors, followed by chemotherapy and tamoxifen, remains the most powerful treatment regimen in not only inducing the BC cell death, but also reducing the bone degradation. The concurrent usage of hormonal therapies (tamoxifen and aromatase inhibitors), without preceding the chemotherapy, was found to have significantly affected the mechanical stimulus compared to the rest of the configurations. So, this treatment regimen can be a better treatment to prevent the key side effect i.e., bone degradation. In terms of treatment doses, increasing the chemotherapy dose has been the most effective method to induce bone osteolysis. The proposed model proved its ability to mimic the BC effect on bone quality and on cancer cells. Further, it also predicted the late effects of these treatments in alignment with the experimental

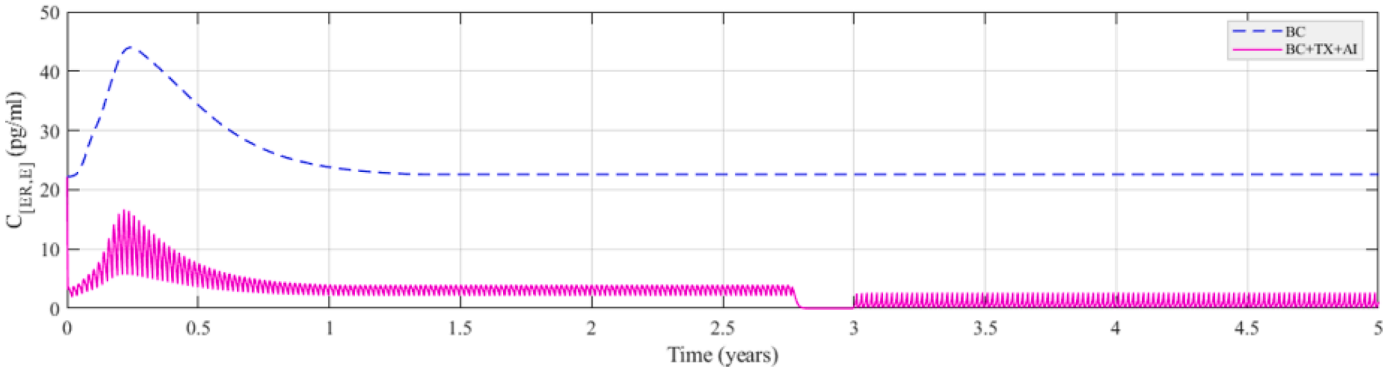

Fig. 8. E-ER concentration in BC cancer case (blue) with tamoxifen and aromatase inhibitors treatments case (pink) over 5 years; the first 3 years were under tamoxifen and the following 2 years were under aromatase inhibitors.

Table 4
Comparison between BDL changes and experimental BMD loss after treatment withdrawal. Chemotherapy (CT), tamoxifen (TX) and aromatase inhibitor (AI).

BC treatment Model simulation BDL	CT 4.91%	Model simulation BDL	CT+TX 5.47%	Model simulation BDL	CT+TX+AI 6.49%	Model simulation BDL	TX+AI 0.82%	Model simulation BDL
Experimental observation BMD loss	5.1%	[53]	5.2%	[57]	6.6%	[54]	0.8%	[58]
	5.6%	[59]	4%	[54]	5.52%	[60]	1%	[58]
	5.8%	[61]						

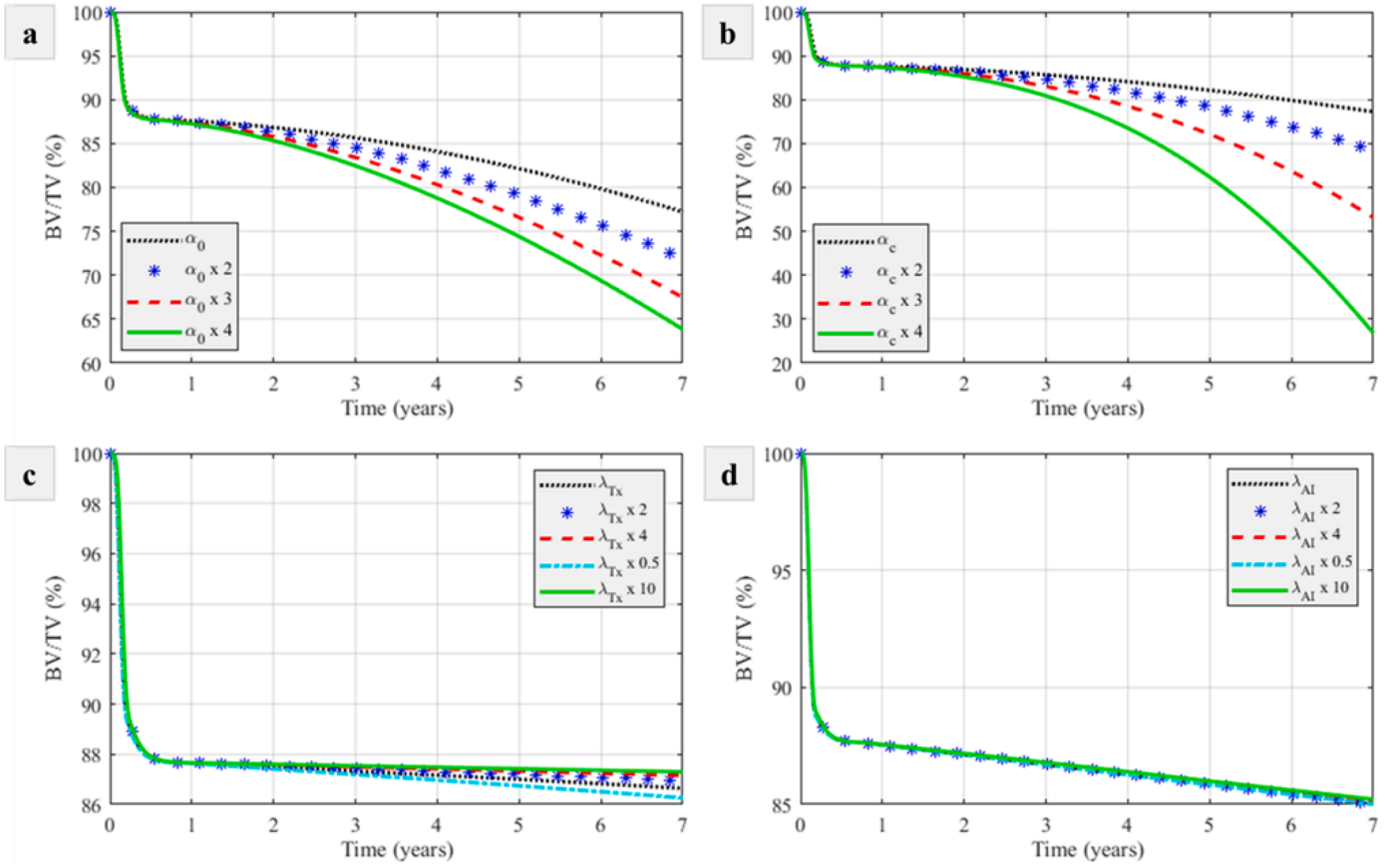

Fig. 9. Parametric study of (a) α_O change influence on BV/TV, (b) α_c change influence on BV/TV, (c) λ_{Tx} change influence on BV/TV, and (d) λ_{AI} change influence on BV/TV.

observations. The proposed model can be further ameliorated with more biological studies on the exact effect of chemotherapy upon the bone cells, by taking the characteristics of a specific bone part into consideration. In the near future, the authors aim at simulating the proposed model using the finite element method and compare the results with that of the scan images captured from the real patients.

Ethics approval statement

Not required

Declaration of Competing Interest

The authors declare no conflict of interest associated with this article.

Acknowledgments

This work was supported by the Partenariat Hubert Curien Franco-Moroccan TOUBKAL (PHC Toubkal) N° TBK/20/102 - CAMPUS N°43681QG.

References

[1] Ait Oumghar I, Barkaoui A, Chabrand P. Toward a mathematical modeling of diseases' impact on bone remodeling: technical review. Front Bioeng Biotechnol 2020:1236. https://doi.org/10.3389/fbioe.2020.584198.
[2] Roodman GD. Pathogenesis of myeloma bone disease. Blood Cells Mol Dis 2004. https://doi.org/10.1016/j.bcmd.2004.01.001.
[3] Muhammad A, Ibrahim M, Erukainure O, Malami I, Sani H, Mohammed H. Metabolism and toxicological implications of commonly used chemopreventive drugs against breast cancer/carcinogenesis. Curr Drug Metab 2017;17:930–6. https://doi.org/10.2174/1389200218666161116121225.
[4] Bouvard B, et al. High prevalence of vertebral fractures in women with breast cancer starting aromatase inhibitor therapy. Ann Oncol 2012. https://doi.org/10.1093/annonc/mdr356.
[5] P. Barry, T. Aspray, K. Briers, and others, "Osteoporosis: assessing the risk of fragility fracture (NICE Clinical Guidance 146," National Institute for Health and Care Excellence, 2012.
[6] Malhotra GK, Zhao X, Band H, Band V. Histological, molecular and functional subtypes of breast cancers. Cancer Biol Therapy 2010;10(10):955–60. https://doi.org/10.4161/cbt.10.10.13879. Cancer Biol TherNov. 15,.

[7] Weigelt B, et al. Refinement of breast cancer classification by molecular characterization of histological special types. J Pathol 2008;216(2):141–50. https://doi.org/10.1002/path.2407. Oct.

[8] Dhankhar R, Vyas SP, Jain AK, Arora S, Rath G, Goyal AK. Advances in novel drug delivery strategies for breast cancer therapy. Artificial cells, blood substitutes, and biotechnology, 38. Artif Cells Blood Substit Immobil Biotechnol; 2010. p. 230–49. https://doi.org/10.3109/10731199.2010.494578. Oct.

[9] Nounou MI, Elamrawy F, Ahmed N, Abdelraouf K, Goda S, Syed-Sha-Qhattal H. Breast cancer: conventional diagnosis and treatment modalities and recent patents and technologies supplementary issue: targeted therapies in breast cancer treatment. Breast Cancer (Auckl) 2015;9(2):17–34. https://doi.org/10.4137/BCBCR.S29420. SupplSep.

[10] Matsen CB, Neumayer LA. Breast cancer: a review for the general surgeon. JAMA surgery, 148. American Medical Association; 2013. p. 971–9. https://doi.org/10.1001/jamasurg.2013.3393.

[11] Tohme S, Simmons RL, Tsung A. Surgery for cancer: a trigger for metastases. Cancer research, 77. American Association for Cancer Research Inc.; 2017. p. 1548–52. https://doi.org/10.1158/0008-5472.CAN-16-1536.

[12] Akram M, Siddiqui SA. Breast cancer management: past, present and evolving. Indian J Cancer 2012;49(3):277–82. https://doi.org/10.4103/0019-509X.104486. Jul.

[13] Jonathan Yang T, Ho AY. Radiation therapy in the management of breast cancer. Surgical clinics of North America, 93. Elsevier; 2013. p. 455–71. https://doi.org/10.1016/j.suc.2013.01.002. Apr. 01.

[14] Colleoni M, et al. Chemotherapy is more effective in patients with breast cancer not expressing steroid hormone receptors: a study of preoperative treatment. Clin Cancer Res 2004;10(19):6622–8. https://doi.org/10.1158/1078-0432.CCR-04-0380. Oct.

[15] Drăgănescu M, Carmocan C. Hormone therapy in breast cancer. Chirurgia (Romania), 112. Editura Celsius; 2017. p. 413–7. https://doi.org/10.21614/chirurgia.112.4.413. Jul. 01.

[16] Muhammad A, et al. Postmenopausal osteoporosis and breast cancer: the biochemical links and beneficial effects of functional foods. Biomed Pharmacother 2018. https://doi.org/10.1016/j.biopha.2018.08.018.

[17] Donaubauer AJ, Deloch L, Becker I, Fietkau R, Frey B, Gaipl US. The influence of radiation on bone and bone cells—differential effects on osteoclasts and osteoblasts. Int J Mol Sci 2020;21(17):1–19. https://doi.org/10.3390/IJMS21176377. Sep.

[18] Wissing MD. Chemotherapy- and irradiation-induced bone loss in adults with solid tumors. Curr Osteoporos Rep 2015;13(3):140. https://doi.org/10.1007/S11914-15-0266-Z. Jun.

[19] Wang Z, et al. Tamoxifen regulates human telomerase reverse transcriptase (hTERT) gene expression differently in breast and endometrial cancer cells. Oncogene 2002;21(22):3517–24. https://doi.org/10.1038/sj.onc.1205463.

[20] Buzdar AU. Pharmacology and pharmacokinetics of the newer generation aromatase inhibitors. Clini Cancer Res 2003;9(1).

[21] Joukar A, Niroomand-Oscuii H, Ghalichi F. Numerical simulation of osteocyte cell in response to directional mechanical loadings and mechanotransduction analysis: considering lacunar–canalicular interstitial fluid flow. Comput Methods Programs Biomed 2016;133:133–41. https://doi.org/10.1016/J.CMPB.2016.05.019. Sep.

[22] Barkaoui A, Ben Kahla R, Merzouki T, Hambli R. Age and gender effects on bone mass density variation: finite elements simulation. Biomech Model Mechanobiol 2017. https://doi.org/10.1007/s10237-016-0834-x.

[23] Komarova SV, Smith RJ, Dixon SJ, Sims SM, Wahl LM. Mathematical model predicts a critical role for osteoclast autocrine regulation in the control of bone remodeling. Bone 2003;33(2):206–15. https://doi.org/10.1016/S8756-3282(03)00157-1.

[24] Pivonka P, et al. Model structure and control of bone remodeling: a theoretical study. Bone 2008;43(2):249–63. https://doi.org/10.1016/j.bone.2008.03.025.

[25] Martínez-Reina J, Pivonka P. Effects of long-term treatment of denosumab on bone mineral density: insights from an in-silico model of bone mineralization. Bone 2019;125:87–95. https://doi.org/10.1016/j.bone.2019.04.022.

[26] Trichilo S, Scheiner S, Forwood M, Cooper DML, Pivonka P. Computational model of the dual action of PTH — application to a rat model of osteoporosis. J Theor Biol 2019;473:67–79. https://doi.org/10.1016/j.jtbi.2019.04.020.

[27] Schön K, Koristkova B, Kacirova I, Brozmanova H, Grundmann M. Comparison of Mw\Pharm 3.30 and Mw\Pharm ++, a Windows version of pharmacokinetic software for PK/PD monitoring of vancomycin. Part 1: a-posteriori modelling. Comput Methods Programs Biomed 2022;214:106552. https://doi.org/10.1016/J.CMPB.2021.106552. Feb.

[28] Savoca A, van Heusden K, Manca D, Ansermino JM, Dumont GA. The effect of cardiac output on the pharmacokinetics and pharmacodynamics of propofol during closed-loop induction of anesthesia. Comput Methods Programs Biomed 2020;192:105406. https://doi.org/10.1016/J.CMPB.2020.105406. Aug.

[29] Lavaill M, Trichilo S, Scheiner S, Forwood MR, Cooper DML, Pivonka P. Study of the combined effects of PTH treatment and mechanical loading in postmenopausal osteoporosis using a new mechanistic PK-PD model. Biomech Model Mechanobiol 2020;19:1765–80. https://doi.org/10.1007/s10237-020-01307-6.

[30] Martin M, Sansalone V, Cooper DML, Forwood MR, Pivonka P. Assessment of romosozumab efficacy in the treatment of postmenopausal osteoporosis: results from a mechanistic PK-PD mechanostat model of bone remodeling. Bone 2020. https://doi.org/10.1016/j.bone.2020.115223.

[31] Ait Oumghar I, et al. Experimental-based mechanobiological modeling of the anabolic and catabolic effects of breast cancer on bone remodeling. Biomech Model Mechanobiol 2022. https://doi.org/10.1007/S10237-022-01623-Z. Aug.

[32] Pastrama MI, Scheiner S, Pivonka P, Hellmich C. A mathematical multiscale model of bone remodeling, accounting for pore space-specific mechanosensation. Bone 2018;107:208–21. https://doi.org/10.1016/j.bone.2017.11.009. May2018.

[33] Scheiner S, Pivonka P, Hellmich C. Coupling systems biology with multiscale mechanics, for computer simulations of bone remodeling. Comput Methods Appl Mech Eng 2013;254:181–96. https://doi.org/10.1016/j.cma.2012.10.015.

[34] Pivonka P, Buenzli PR, Scheiner S, Hellmich C, Dunstan CR. The influence of bone surface availability in bone remodelling-A mathematical model including coupled geometrical and biomechanical regulations of bone cells. Eng Struct 2013;47:134–47. https://doi.org/10.1016/j.engstruct.2012.09.006.

[35] Buenzli P, Pivonka P, Gardiner B, Smith D. Modelling the anabolic response of bone using a cell population model. J Theor Biol 2012;307:42–52. https://doi.org/10.1016/J.JTBI.2012.04.019. Aug.

[36] Wang Y, Pivonka P, Buenzli PR, Smith DW, Dunstan CR. Computational modeling of interactions between multiple myeloma and the bone microenvironment. PLoS ONE 2011;6:e27494. https://doi.org/10.1371/journal.pone.0027494.

[37] Pivonka P, et al. Model structure and control of bone remodeling: a theoretical study. Bone 2008. https://doi.org/10.1016/j.bone.2008.03.025.

[38] Khattar D, Sodhi C, Parmod J, Dutta A. Correlating estrogen levels and cognitive functions in regularly menstruating females of reproductive age group and post menopausal women of North India. J Family Reprod Health 2015;9(2):83. https://doi.org/10.18035/emj.v3i1.266. Apr.

[39] Smith JW, et al. Phase II randomized trial of weekly and every-3-week ixabepilone in metastatic breast cancer patients. Breast Cancer Res Treat 2013;142(2):381–8. https://doi.org/10.1007/S10549-013-2742-4. Nov.

[40] Ibrahim NK. Ixabepilone: overview of effectiveness, safety, and tolerability in metastatic breast cancer. Front Oncol 2021;11. https://doi.org/10.3389/FONC.2021.617874. Jul.

[41] Buzdar AU, et al. Bioequivalence of 20-mg once-daily tamoxifen relative to 10-mg twice-daily tamoxifen regimens for breast cancer. J Clin Oncol 1994;12(1):50–4. https://doi.org/10.1200/JCO.1994.12.1.50.

[42] Untch M, Jackisch C. Exemestane in early breast cancer: a review. Ther Clin Risk Manag 2008;4(6):1295. https://doi.org/10.2147/TCRM.S4007.

[43] Kittaneh M, Glück S. Exemestane in the adjuvant treatment of breast cancer in postmenopausal women. Breast Cancer (Auckl) 2011;5(1). https://doi.org/10.4137/BCBCR.S6234.

[44] EMA. Withdrawal assessment report for ixempra (ixabepilone). EMEA/594033/2008. EMA - Committee for Medicinal Products for Human Use; 2009.

[45] Dahmane EBA. Tamoxifen pharmacokinetics and pharmacogenetics. Endocrine Sensitive Breast Cancer Patients; 2013. p. 1–184.

[46] Valle M, et al. A predictive model for exemestane pharmacokinetics/pharmacodynamics incorporating the effect of food and formulation. Br J Clin Pharmacol 2005;59(3):355. https://doi.org/10.1111/J.1365-2125.2005.02335.X. Mar.

[47] Hubert F, Leszczyński M, Ledzewicz U, Schättler H. Optimal control for a mathematical model for chemotherapy with pharmacometrics. Math Model Nat Phenom 2020;15. https://doi.org/10.1051/MMNP/2020008.

[48] Mager DE, Jusko WJ. General pharmacokinetic model for drugs exhibiting target-mediated drug disposition. J Pharmacokinet Pharmacodyn 2001;28(6):507–32. https://doi.org/10.1023/A:1014414520282.

[49] J.I. Osotsi, "Mathematical modelling of the efficacy and toxicity of cancer chemotherapy," 2017.

[50] Oke SIsaac, Matadi M, Xulu S. Optimal control analysis of a mathematical model for breast cancer. Math Comput Appl 2018;23(2):21. https://doi.org/10.3390/mca23020021.

[51] Rich RL, et al. Kinetic analysis of estrogen receptor/ligand interactions. Proc Natl Acad Sci 2002;99(13):8562–7. https://doi.org/10.1073/PNAS.142288199. Jun.

[52] Saarto T, Blomqvist C, Välimäki M, Mäkelä P, Sarna S, Elomaa I. Chemical castration induced by adjuvant cyclophosphamide, methotrexate, and fluorouracil chemotherapy causes rapid bone loss that is reduced by clodronate: a randomized study in premenopausal breast cancer patients. J Clin Oncol 1997;15(4):1341–7. https://doi.org/10.1200/JCO.1997.15.4.1341.

[53] Vehmanen L, Saarto T, Elomaa I, Mäkelä P, Välimäki M, Blomqvist C. Long-term impact of chemotherapy-induced ovarian failure on bone mineral density (BMD) in premenopausal breast cancer patients. The effect of adjuvant clodronate treatment. Eur J Cancer 2001;37(18):2373–8. https://doi.org/10.1016/S0959-8049(01)00317-3.

[54] Bouvard B, et al. French recommendations on strategies for preventing and treating osteoporosis induced by adjuvant breast cancer therapies. Joint Bone Spine 2019. https://doi.org/10.1016/j.jbspin.2019.07.005.

[55] Sugiyama T, Galea GL, Lanyon LE, Price JS. Mechanical loading-related bone gain is enhanced by tamoxifen but unaffected by fulvestrant in female mice. Endocrinology 2010;151(12):5582–90. https://doi.org/10.1210/EN.2010-0645. Dec.

[56] Lønning PE, Johannessen DC, Lien EA, Ekse D, Fotsis T, Adlercreutz H. Influence of tamoxifen on sex hormones, gonadotrophins and sex hormone binding globulin in postmenopausal breast cancer patients. J Steroid Biochem Mol Biol 1995;52(5):491–6. https://doi.org/10.1016/0960-0760(94)00189-S. May.

[57] Cohen A, et al. Prevention of bone loss after withdrawal of tamoxifen. Endocr Pract 2008;14(2):162. https://doi.org/10.4158/EP.14.2.162.

[58] Coleman RE, et al. Skeletal effects of exemestane on bone-mineral density, bone biomarkers, and fracture incidence in postmenopausal women with early breast cancer participating in the Intergroup Exemestane Study (IES): a randomised controlled study. Lancet Oncol 2007;8(2):119–27. https://doi.org/10.1016/S1470-2045(07)70003-7. Feb.

[59] Hadji P, Ziller M, Maskow C, Albert U, Kalder M. The influence of chemotherapy on bone mineral density, quantitative ultrasonometry and bone turnover in pre-menopausal women with breast cancer. Eur J Cancer 2009;45(18):3205–12. https://doi.org/10.1016/J.EJCA.2009.09.026. Dec.

[60] Kalder M, Hadji P. Breast cancer and osteoporosis – management of cancer treatment-induced bone loss in postmenopausal women with breast cancer. Breast Care 2014;9(5):312. https://doi.org/10.1159/000368843. Dec.

[61] Monroy-Cisneros K, et al. Antineoplastic treatment effect on bone mineral density in Mexican breast cancer patients. BMC Cancer 2016;16(1). Nov.0.1186/S12885-016-2905-X.